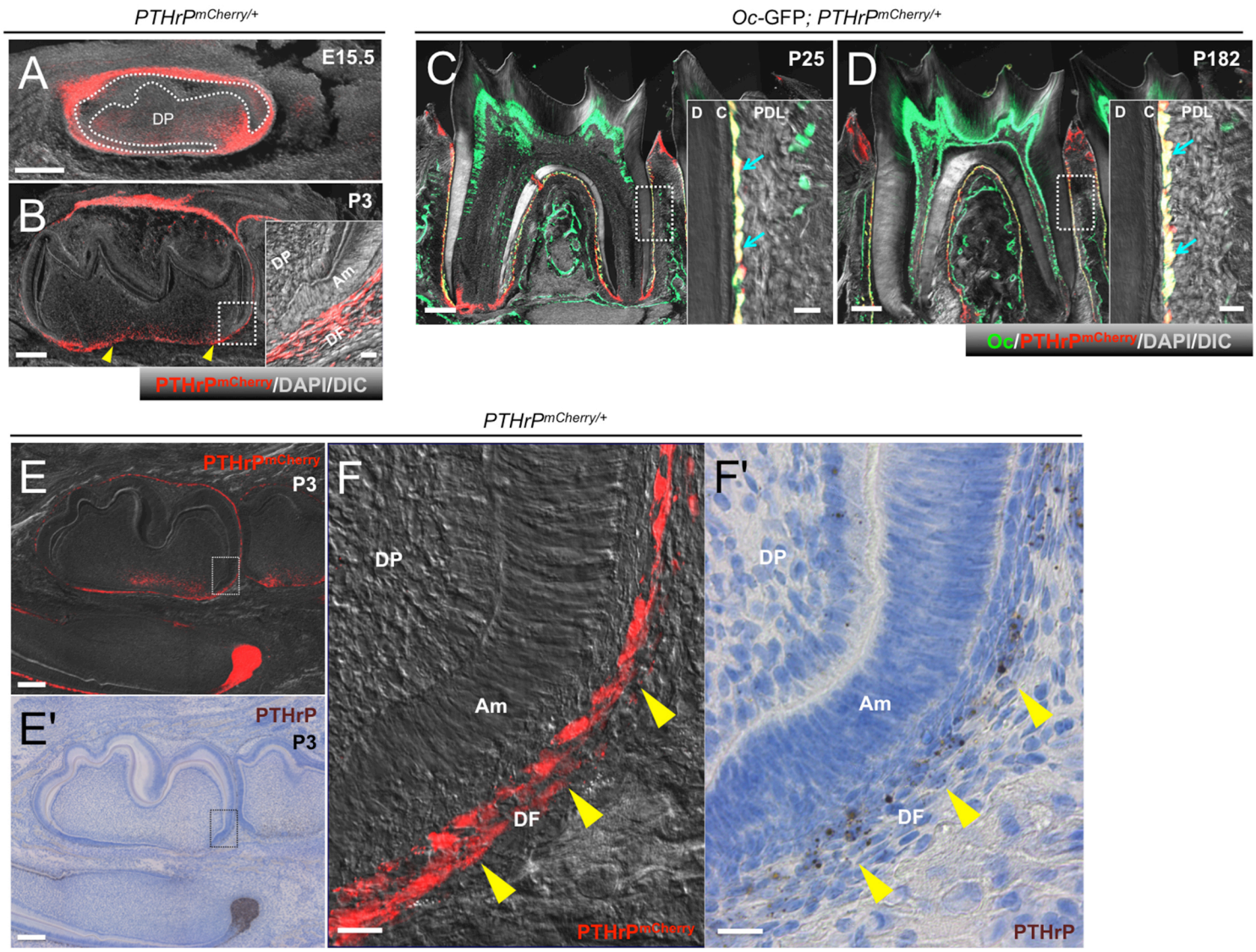

Figure S1. Characterization of *PTHrP*-mCherry⁺ dental follicle cells.

(A-D) *PTHrP*-mCherry expression in dental follicle (A,B) and cementoblasts (C,D). DP: dental papilla, DF: dental follicle, Am: ameloblasts. Arrowheads: mCherry⁺ DF cells. D: dentin, C: cementum, PDL: periodontal ligament. Arrows: GFP⁺mCherry⁺ cementoblasts. Scale bars: 200μm, 20μm (insets).
(E,F) RNAscope in situ hybridization assay for *PTHrP* mRNA. (E,F): mCherry fluorescence signal before hybridization, (E',F'): after hybridization. DP: dental papilla, DF: dental follicle, Am: ameloblasts. Arrowheads: *PTHrP*⁺mCherry⁺ DF cells.

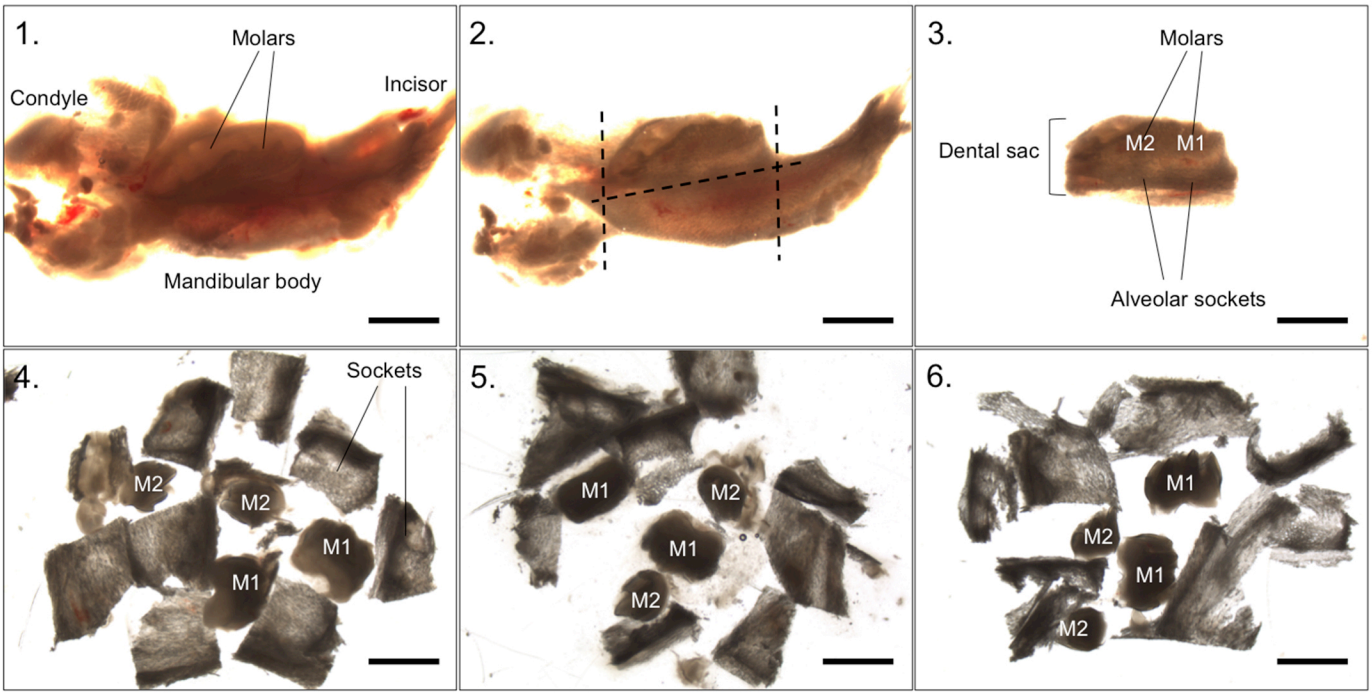

Figure S2. A cell dissociation protocol to harvest cells highly enriched for dental follicle cells.

Protocol for harvesting cells highly enriched for dental follicle mesenchymal cells.

(1) The mandible was carefully detached from the skull first, and the symphysis was excised to separate each side of the mandible.

(2) The gingival tissue (oral epithelium) was completely removed using sharp forceps, and the dentoalveolar component (the area containing molars, alveolar sockets and dental sacs) was carefully resected using a scalpel.

(3) After the resection. Note that this component is completely free from epithelial tissues.

(4) In a new well containing digestion solution containing Liberase (2Wu), the molars (M1 and M2) were carefully extracted from the sockets.

(5) After the digestion at 37^{o}C for 15 min. Note that only the dental sac was dissociated by this short digestion, without any notable digestion of the molars or the sockets. (6) Dental follicle cells were aspirated by rigorous pipetting. Scale bars: 300μm.

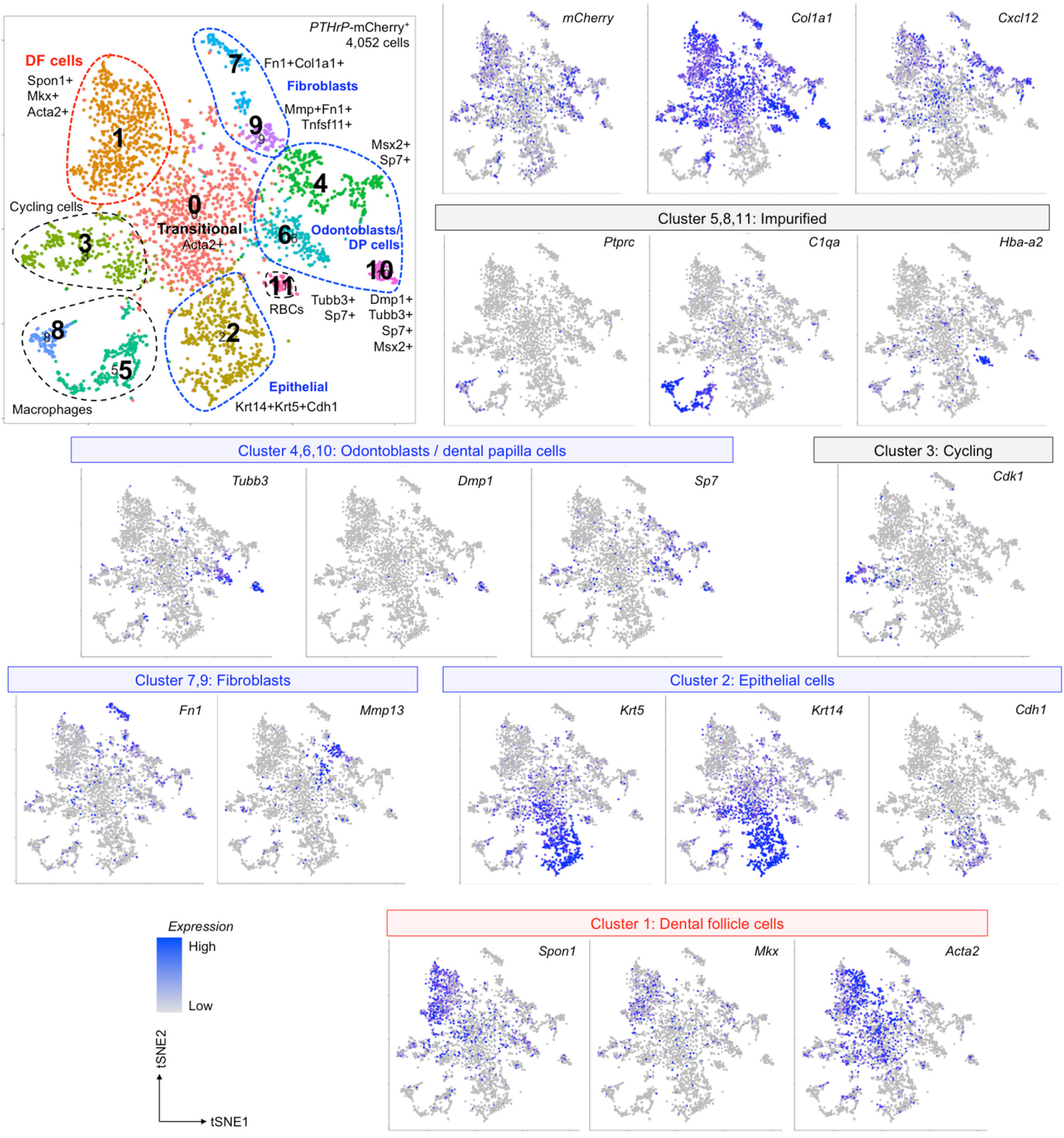

Figure S3. A single cell RNA-seq analysis of *PTHrP*-mCherry⁺ cells.

t-SNE-based visualization of major classes of FACS-sorted *PTHrP*-mCherry⁺ single cells at P6 (Cluster 0-11). Cluster 0: transitional cells, Cluster 1: dental follicle (DF) cells, Cluster 2: epithelial cells, Cluster 3: cycling cells, Cluster 4,6,10: odontoblasts and dental papilla (DP) cells, Cluster 5,8,11: impurified cells (hematopoietic cells without mCherry expression), Cluster 7,9: fibroblasts. Dots: individual cells, color: cell type. Feature plots: expression of the indicated gene. Blue: high expression, grey: no expression. *n*=4,052 cells.

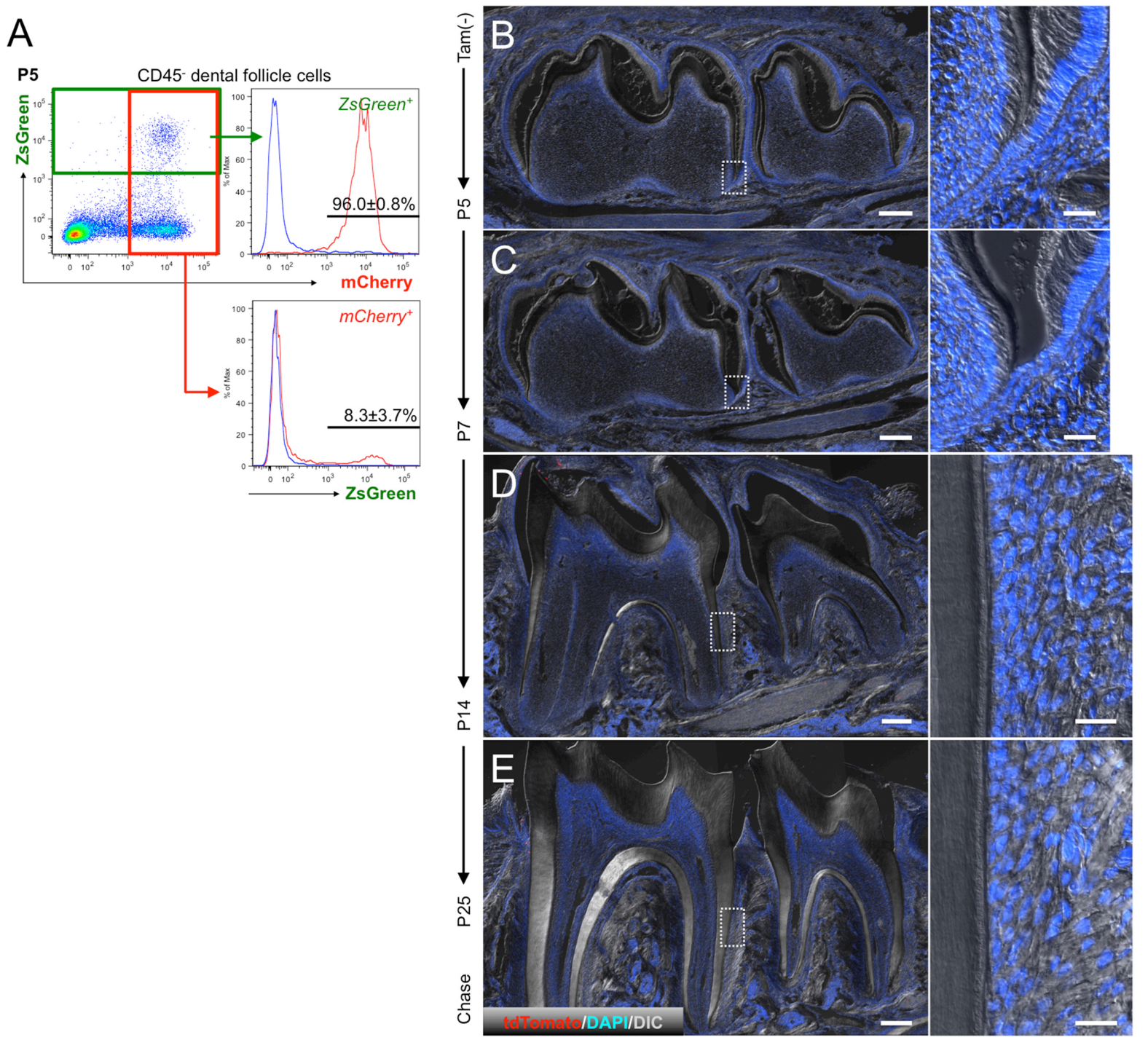

Figure S4. Characterization of dental follicle-specific *PTHrP-creER* line.

(A) Flow cytometry analysis of P5 *PTHrP*$^{mCherry/+}$; *PTHrP-creER*; *R26R*^{ZsGreen} dental follicle cells (tamoxifen at P3). *x* axis: mCherry, *y* axis: ZsGreen. Right upper panel: CD45$^-$CD31$^-$Ter119$^-$ZsGreen$^+$ fraction developed for mCherry (red line). *x* axis: mCherry. Blue line: *PTHrP*$^{+/+}$; *PTHrP-creER*; *R26R*^{ZsGreen} (tamoxifen at P3) control dental follicle cells. Right lower panel: CD45$^-$CD31$^-$Ter119$^-$mCherry$^+$ fraction developed for ZsGreen (red line). *x* axis: ZsGreen, Blue line: *PTHrP*$^{mCherry/+}$; *R26R*^{ZsGreen} control dental follicle cells. *y* axis: percentage of maximum. *n*=4 mice.
(B-E) *PTHrP-creER*; *R26R*^{Tomato} mandibular first molars (M1) at P5 (B), P7 (C), P14 (D) and P25 (E) without tamoxifen injection. Right panels: magnified views of M1 distal periodontal space. Red: tdTomato, blue: DAPI, gray: DIC. Scale bars: 200μm, 20μm (insets).

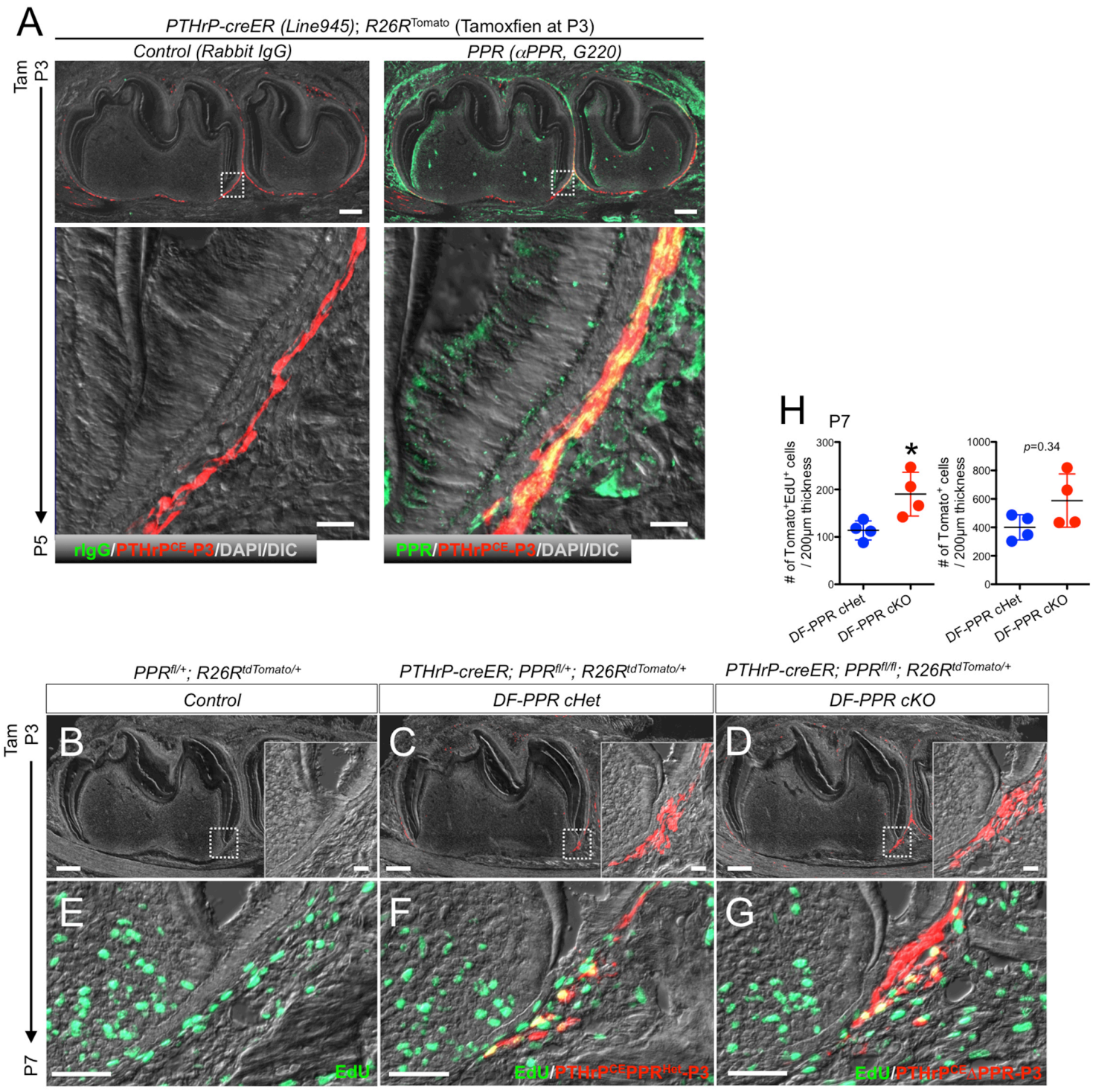

Figure S5. PTHrP-PPR autocrine signaling orchestrates periodontal ligament differentiation of dental follicle mesenchymal progenitor cells *in vivo*.

(A) PPR staining for P5 *PTHrP-creER*; *R26R*^{Tomato} mandibular molars (tamoxifen at P3). Left panels: isotype control, lower panels: magnified views of dotted areas in upper panels. Green: αPPR-Alexa488, red: tdTomato, gray: DAPI and DIC. Scale bars: 200μm (upper), 20μm (lower).
(B-G) Mandibular first molars (M1) of (B,E) *PPR*$^{fl/+}$; *R26R*^{Tomato} (Control), (C,F) *PTHrP-creER*; *PPR*$^{fl/+}$; *R26R*^{Tomato} (DF-PPR cHet) and (D,G) *PTHrP-creER*; *PPR*$^{fl/fl}$; *R26R*^{Tomato} (DF-PPR cKO) mice at P7 (tamoxifen at P3). Insets in (B-D): magnified views of the dotted areas. (E-G): EdU was administered twice (6 and 3 hrs) prior to analysis. Sections were stained for EdU. Green: EdU-Alexa488, red: tdTomato, grey: DAPI and DIC. Scale bars: 200μm, 20μm (insets, B-D), 50μm (E-G).
(H) Quantifications of tdTomato$^+$EdU$^+$ cells and tdTomato$^+$ cells at P7. *p<0.05, Mann–Whitney's U-test. All data are represented as mean ± S.D.

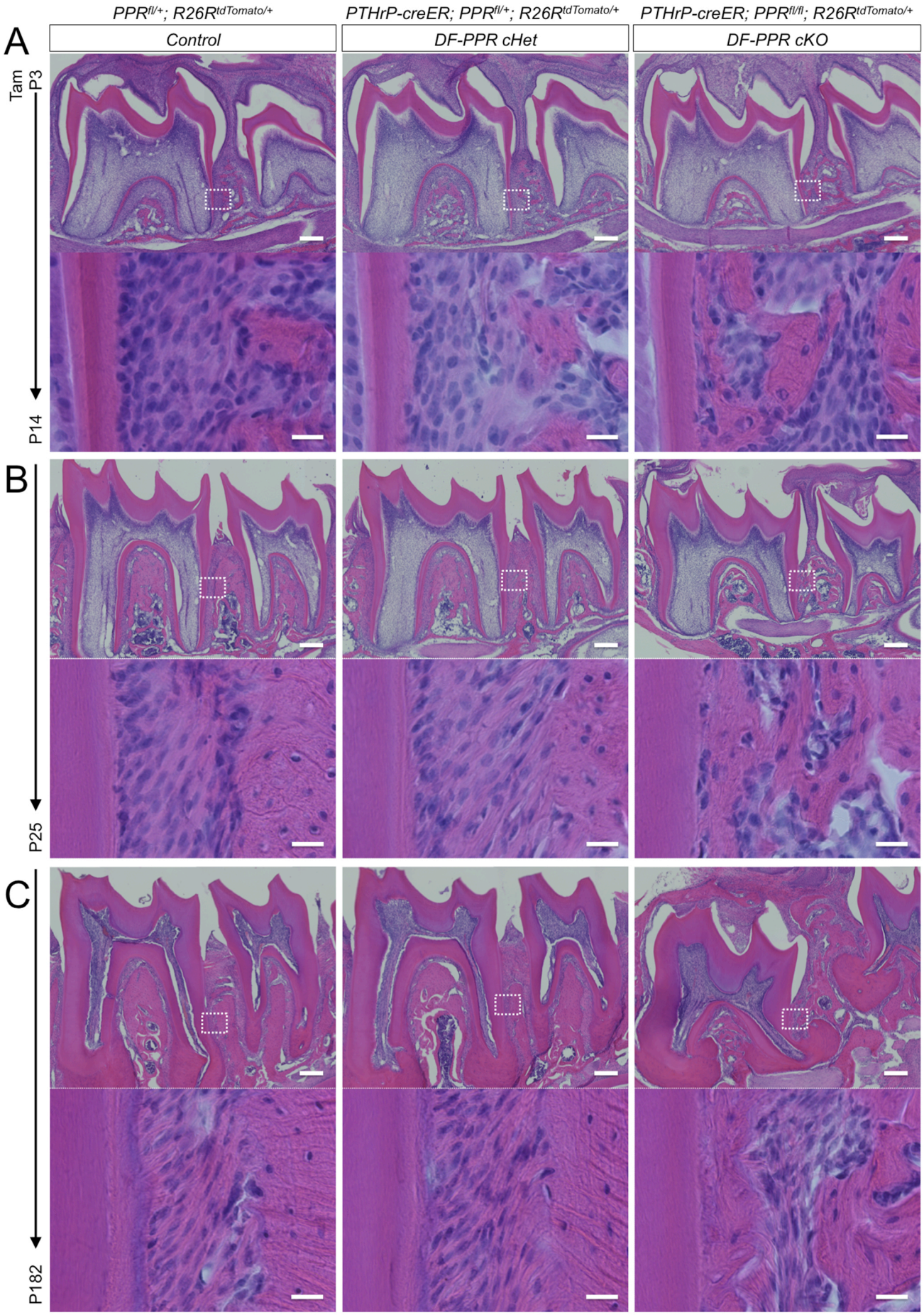

Figure S6. Tooth root anomalies associated with *PTHrP-creER*$^{+}$ DF-specific PPR-deficiency. Mandibular first molars (M1) of *PPR*$^{fl/+}$; *R26R*^{Tomato} (Control, left panels), *PTHrP-creER*; *PPR*$^{fl/+}$; *R26R*^{Tomato} (DF-PPR cHet, center panels) and *PTHrP-creER*; *PPR*$^{fl/fl}$; *R26R*^{Tomato} (DF-PPR cKO, right panels) mice at P14 (A), P25 (B) and P182 (C) stained for hematoxylin and eosin. Lower panels: magnified views of the dotted areas. Scale bars: 200μm, 20μm (insets).

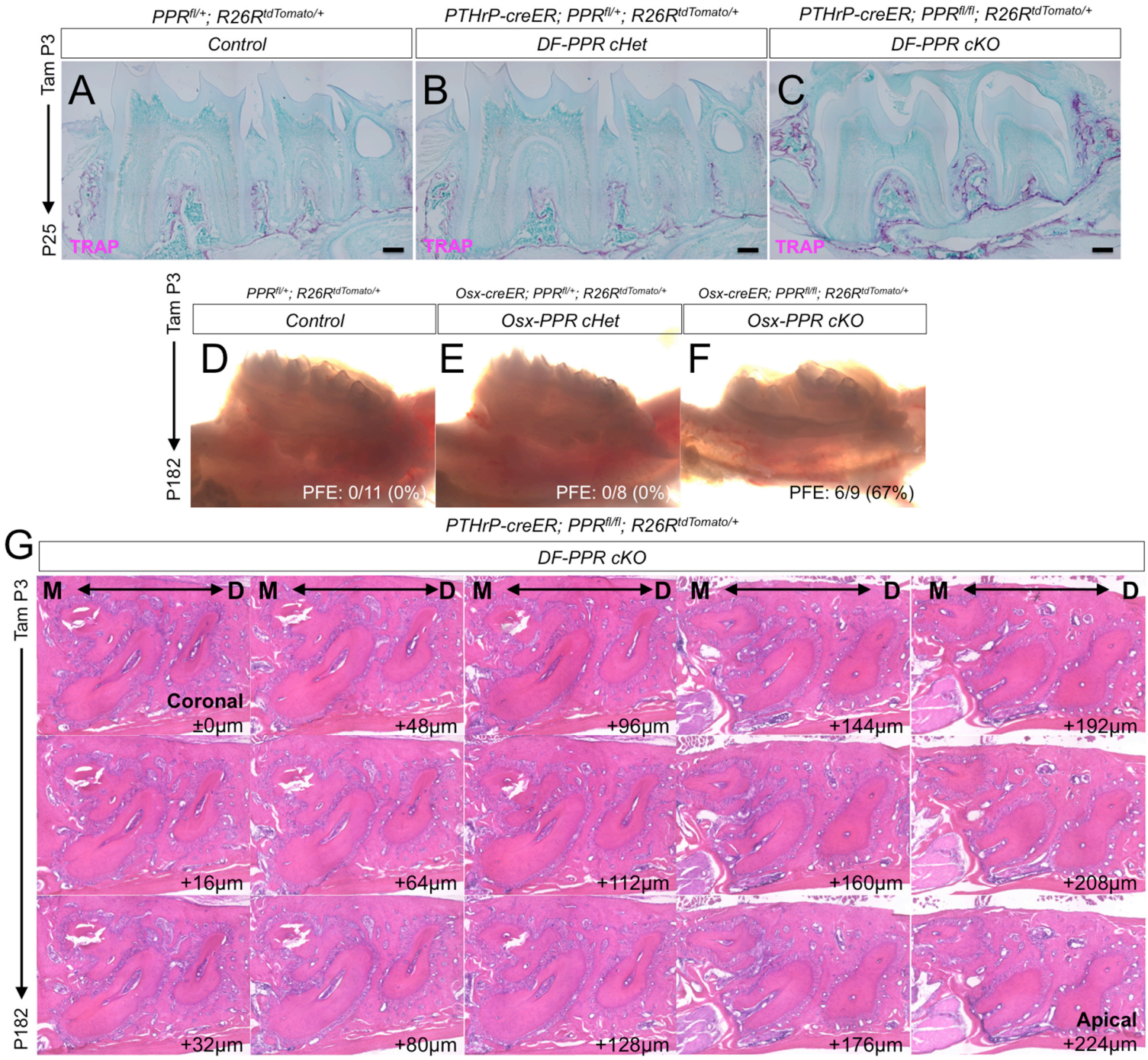

Figure S7. TRAP staining, and primary failure of eruption phenotypes caused by PPR-deficiency in *Osx-creER*$^{+}$ dental mesenchymal cells.

(A-C) Mandibular first molars (M1) of (A) *PPR*$^{fl/+}$; *R26R*^{Tomato} (Control), (B) *PTHrP-creER*; *PPR*$^{fl/+}$; *R26R*^{Tomato} (DF-PPR cHet) and (C) *PTHrP-creER*; *PPR*$^{fl/fl}$; *R26R*^{Tomato} (DF-PPR cKO) mice at P25 (tamoxifen at P3). Sections were stained for TRAP activities. Scale bars: 200μm.
(D-F) Stereoscopic images of (D) Control, (E) Osx-PPR cHet and (F) DF-PPR cKO molars at 6 months of age (tamoxifen at P3). Quantification shows the incidence of failure of eruption (lack of gingival perforation).
(G) Serial horizontal sections of *PTHrP-creER*; *PPR*$^{fl/fl}$; *R26R*^{Tomato} (DF-PPR cKO) M1 roots at P182 (tamoxifen at P3). Sections were stained for H&E.

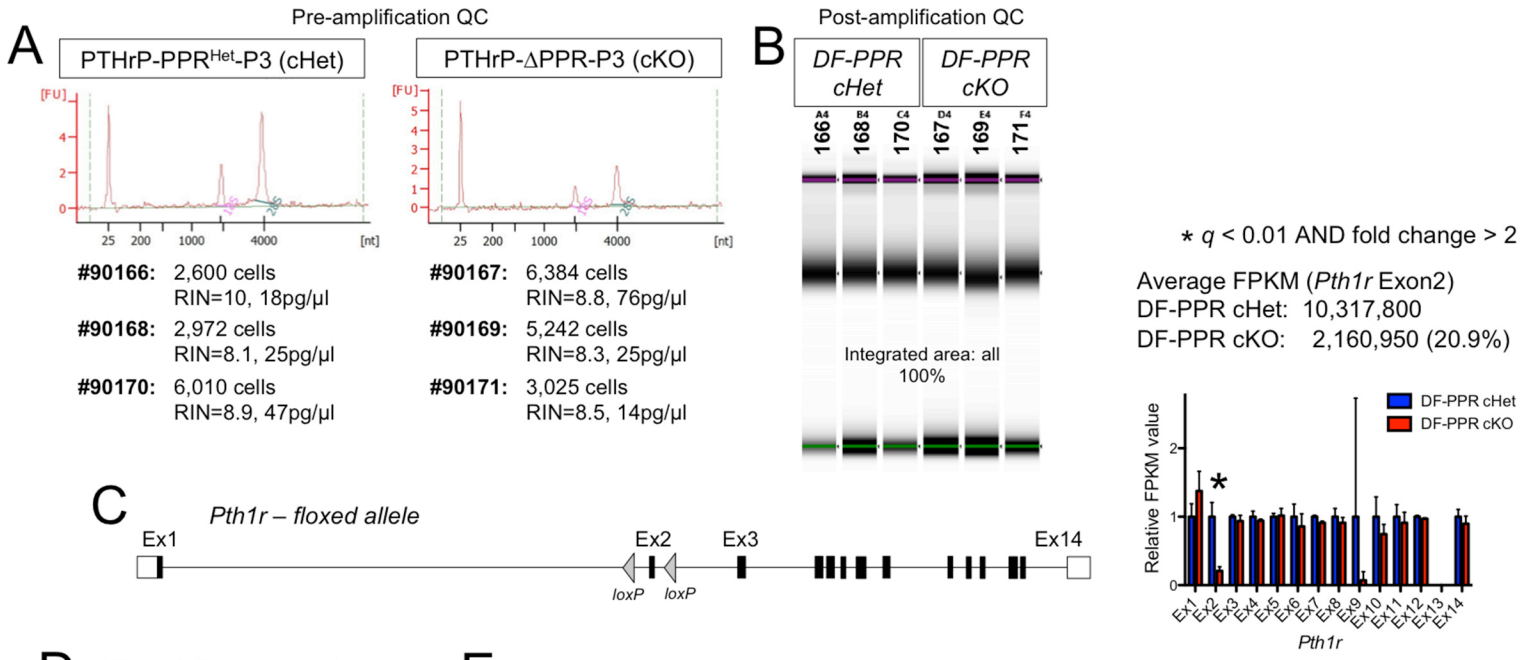

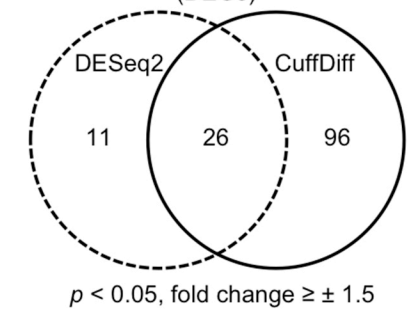

26 genes:
Up in cKO (23): Col13a1, Dmp1, Loxl4, Col2a1, Cdo1, Ramp1, Arhgef26, Ptgis, Pde1b, Cd200, Coch, Gucy1a3, Stmn2, Prss35, Tnfrsf11b, Rasa3, Prex1, Dtx4, Nrtn, Sgms2, Pdgfa, Myo1b, Spp1
Down in cKO (3): Tgfbi, Stbd1, Vipr2

E

GOterm – Biological process: Enrichment analysis of DEGs

goId	goName	countDE	countAll	pv_elim
GO:0031214	biomineral tissue development	8	127	0.00033
GO:0050714	positive regulation of protein secretion	7	234	0.00233
GO:0006935	chemotaxis	11	492	0.00279
GO:0006954	inflammatory response	9	587	0.00792
GO:0010975	regulation of neuron projection development	12	485	0.00849
GO:0032956	regulation of actin cytoskeleton organization	7	287	0.0105
GO:0001525	angiogenesis	7	428	0.01341
GO:0010001	glial cell differentiation	6	201	0.01694
GO:0045666	positive regulation of neuron differentiation	8	370	0.01844
GO:0043410	positive regulation of MAPK cascade	10	440	0.01888
GO:0071363	cellular response to growth factor stimulus	10	513	0.01936
GO:0042592	homeostatic process	25	1580	0.01992
GO:0007155	cell adhesion	22	1436	0.02153
GO:0008285	negative regulation of cell proliferation	8	611	0.02806
GO:0048534	hematopoietic or lymphoid organ development	11	870	0.0301
GO:0016477	cell migration	19	1173	0.03035
GO:0045937	positive regulation of phosphate metabolic process	22	996	0.03464
GO:0042060	wound healing	6	332	0.04434
GO:0030855	epithelial cell differentiation	11	565	0.04792

Figure S8. RNA-seq analysis of PPR-deficient *PTHrP-creER*$^+$ DF cells.
(A) Pre-amplification quality control results of RNA samples. Shown are Bioanalyzer traces (28S/18S) of PTHrP-PPR^{Het}-P3 (cHet, left panel) and PTHrP-ΔPPR-P3 (cKO, right panel). Cell numbers, RINs (RNA integrity numbers) and concentrations (pg/μl) of each sample are also shown. *n*=3 mice per group.
(B) Post-amplification quality control results of cDNA samples. Shown are TapeStation gel images of PTHrP-PPR^{Het}-P3 (cHet, left lanes) and PTHrP-ΔPPR-P3 (cKO, right lanes). All samples demonstrated the integrate area of 100%.
(C) Diagram of *Pth1r* floxed allele. Exon 2 is flanked by *loxP* sites and excised upon *cre* recombination. Lower panel: Relative FPKM values of exon 1 – 14 of *Pth1r* gene. FPKM values of PTHrP-ΔPPR-P3 (cKO) were normalized to those of PTHrP-PPR^{Het}-P3 (cHet) on each exon. Exon 13 did not show any FPKM. Only exon 2 showed statistical significance and fold change greater than two. *q<0.05 and fold change > 2
(D) Venn diagram of differentially expressed genes (DEGs) determined by DESeq2 (dotted circle) and CuffDiff (solid circle) software, based on the criteria of p < 0.05 and fold change ≥ ± 1.5. DESeq2 and CuffDiff software identified 37 and 122 DEGs, respectively, of which 26 genes were in common. The list of the 26 genes is shown below; 23 genes were upregulated, while 3 genes were downregulated in PTHrP-ΔPPR-P3 (cKO).
(E) Gene Ontology (GO) terms / Biological Processes that are overrepresented in DEGs (p<0.05, minimum DEGs=6).

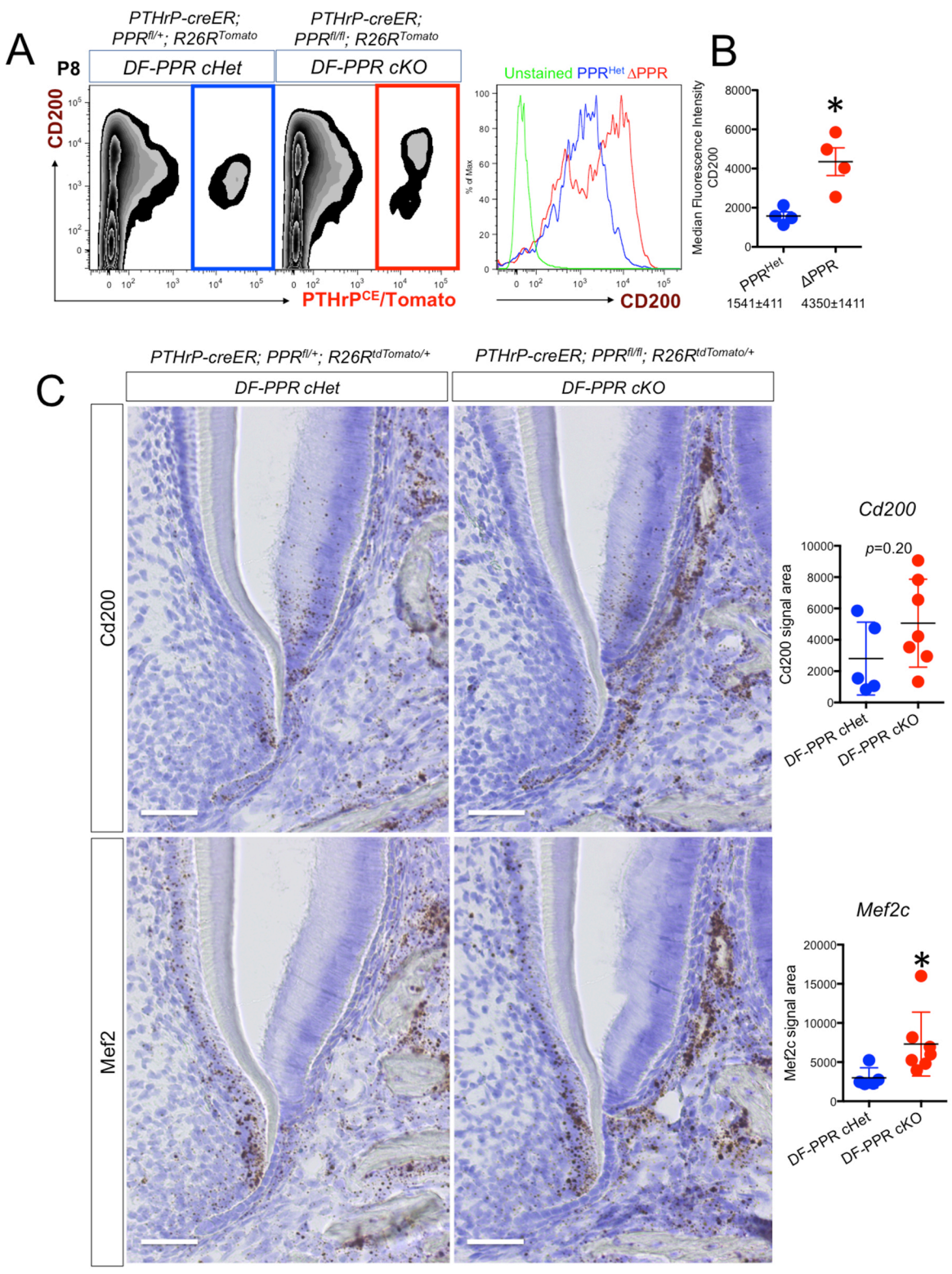

Figure S9. Validation of *Cd200* and *Mef2c* upregulation in PPR-deficient *PTHrP-creER*$^{+}$ dental follicle cells.

(A,B) Flow cytometry analysis of dental follicle cells stained for CD200. (B): Median fluorescent intensity (MFI) of CD200. *p<0.05, Mann–Whitney's U-test. All data are represented as mean ± S.D. **(C)** RNAscope analysis of *PTHrP-creER*; *PPR*$^{fl/+}$; *R26R*^{Tomato} (DF-PPR cHet, left panel) and *PTHrP-creER*; *PPR*$^{fl/fl}$; *R26R*^{Tomato} (DF-PPR cKO, right panel) molars at P8 (tamoxifen at P3). Upper panels: *Cd200*, lower panels: *Mef2c*. Brown: DAB, blue: hematoxylin. Scale bars: 50µm. Right panels: quantification of DAB signal areas. n=5 for DF-PPR cHet, n=7 for DF-PPR cKO. *p<0.05, Mann–Whitney's U-test. All data are represented as mean ± S.D.

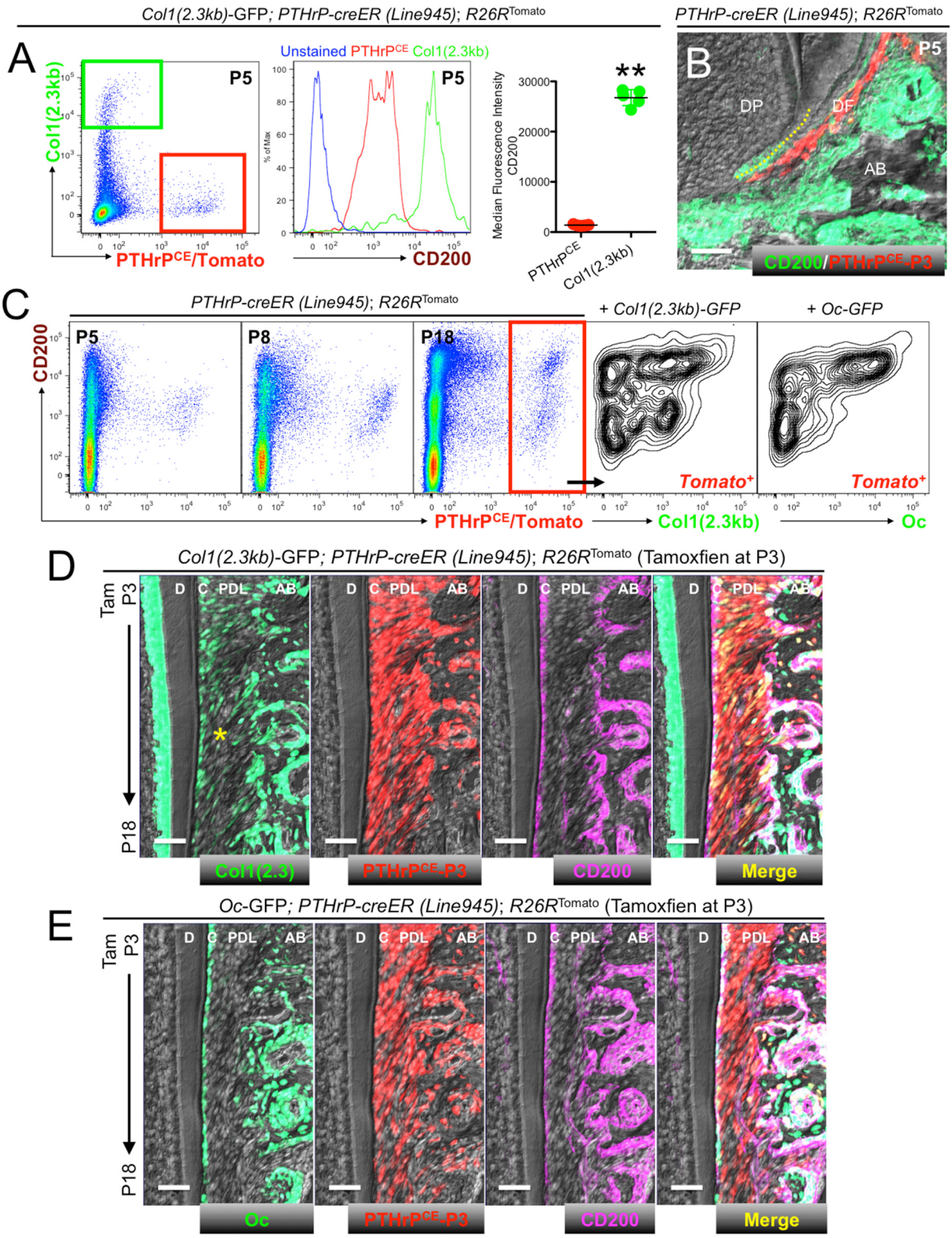

Figure S10. Expression of CD200 in dental follicle, PDL fibroblasts, cementoblasts and osteoblasts.

(A) Flow cytometry analysis of P5 dental follicle cells. Right panel: Median fluorescent intensity (MFI) of CD200. *p<0.05, Mann–Whitney's U-test. All data are represented as mean ± S.D.
(B) CD200 staining. DP: dental papilla, DF: dental follicle, AB: alveolar bone. Yellow dotted line: Hertwig's epithelial root sheath (HERS). Scale bars: 50μm.
(C) Flow cytometry analysis of dental follicle cells at P5 (leftmost), P8 (left center) and P18 (center and right panels), stained for CD200.
(D,E) M1 distal periodontal space of (D) *Col1(2.3kb)*-GFP; *PTHrP-creER*; *R26R*^{Tomato} and (E) *Oc*-GFP; *PTHrP-creER*; *R26R*^{Tomato} mice at P18 (tamoxifen at P3). Sections were stained for CD200. D: dentin, C: cementum, PDL: periodontal ligament, AB: alveolar bone. Green: periostin-Alexa488, red: tdTomato, magenta: CD200-Alexa633, gray: DAPI and DIC. Scale bars: 50μm.

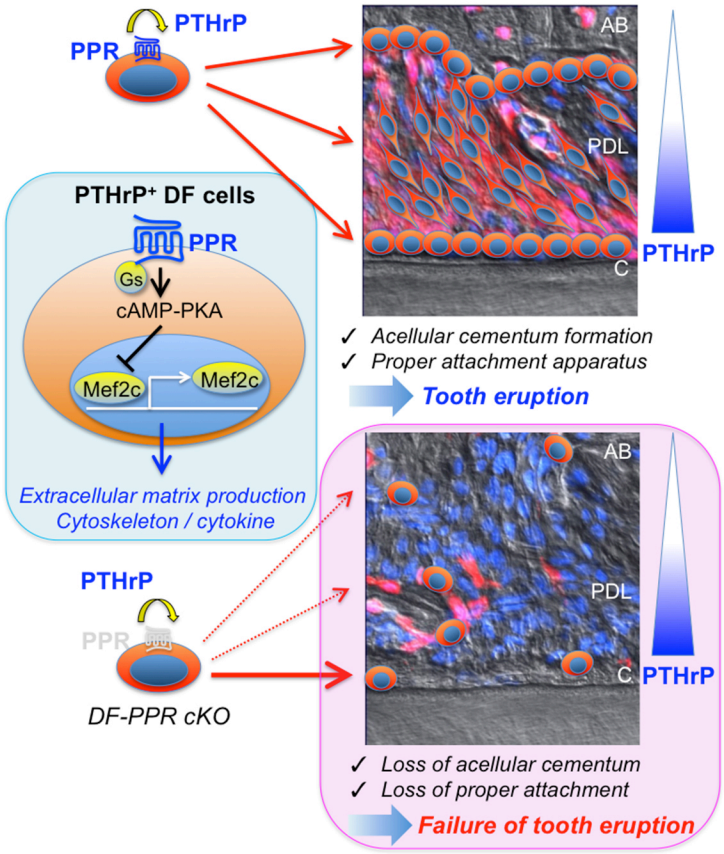

Figure S11. Autocrine regulation of mesenchymal progenitor cell fates orchestrates tooth eruption.

Concluding diagram of this study. PTHrP-PPR autocrine signaling in DF progenitor cells is essential to maintaining their proper cell fates by suppressing Mef2c autoregulation circuit, which coordinates extracellular matrix production, cytoskeleton formation and cytokine regulation. The resultant functional periodontal attachment apparatus with acellular cementum is important for tooth eruption. Defective PTHrP-PPR signaling in these progenitor cells leads to improper cell fates, loss of functional periodontal attachment and failure of tooth eruption. AB: alveolar bone, PDL: periodontal ligament, C: cementum. Reverse triangle: gradient of PTHrP in periodontal space.

Supplemental Methods

Generation of *PTHrP*^{mCherry} knock-in allele by CRISP/Cas9 technology.

An mCherry reporter allele of the *PTHrP* gene was generated by replacing the native start codon in exon 2 with a *Kozak*-mCherry-*bGHpA* cassette with CRISP/Cas9 technology, as reported previously(1). A single guide RNA (sgRNA) target and a protospacer adjacent motif (PAM) were identified near the start codon. The sgRNA target was cloned into plasmid pX330 (Addgene.org, plasmid #42230). The guide targets were C32G1: 5' GCTACTCCGTGCCCTCCCGC 3' PAM: GGG. A DNA donor was synthesized (Invitrogen GeneArt ThermoFisher.com) to replace the start codon and following 58 nucleotides with the following elements: ggtgg – mCherry cDNA (GenBank Accession Number AF506027) – bovine growth hormone polyadenylation signal. The DNA donor included a 1,688 bp 5' arm of homology and a 331 bp 3' arm of homology. The DNA donor was designed so that it did not include the C32G1 sgRNA targets.

Potential G0 mouse founders carrying the *PTHrP*^{mCherry} knock-in allele were produced by pronuclear microinjection of fertilized mouse eggs obtained by mating B6SJLF1 female mice with B6SJLF1 male mice (Jackson Laboratory stock number 100012, Bar Harbor, ME). Fertilized eggs were microinjected with circular plasmid pX330 expressing sgRNA C32G1 (5 ng/µl) and 10 ng/µl of the circular DNA donor plasmid. Following microinjection, eggs were transferred to pseudopregnant females. Genomic DNA from potential G0 mouse founders were initially screened by PCR, using 5' primers (341: GGGAAAGAGACAAGGGCTTC, 342: CGCATGAACTCCTTGATGAT, 1,785bp) and 3' primers (343: ACGACTGTGCCTTCTAGTTGC, 344: AGTTTCAGAACCTCTCGGTGGA, 582bp), in which one primer is designed external to homology arms while another primer is designed internal to the transgene. Generic mCherry primers (339: CCTGTCCCCTCAGTTCATGT, 340: CCCATGGTCTTCTTCTGCAT, 240bp) were also used.

The PCR-positive G0 founder was identified and was further backcrossed with C57/BL6 mice at least for three generations to remove potential off-target events. Mice were genotyped using PCR primers (378 Pthlh Int1 Fw: ACTTGTGAGATGCCCTCGAC, 379 Pthlh Ex2 Rv: CAGGACACTCCACTGCTGAA and 380 mRFP Rv: ACATGAACTGAGGGGACAGG, 185bp for wild-type, 368bp for mCherry allele).

PTHrP-creER bacterial artificial chromosome (BAC) transgenic mice.

PTHrP-creER-WPRE-rGHpA transgenic mice were generated by pronuclear injection of a modified bacterial artificial chromosome (BAC) clone RP23-27F7 (Children's Hospital Oakland Research Institute, Oakland, CA) containing 131kb upstream and 82kb downstream genomic sequences of the *PTHrP* gene, as reported previously(1). A *creER*^{T2}-*WPRE-rGHpA-frt-Neo*^{R}*-frt* (CEWrAfN) plasmid was constructed by subcloning an *frt-Neo-frt* sequence, which was PCR-amplified from a *pCS2.frt.Neo* plasmid, into the PstI site, and by replacing an EGFP with a *creER*^{T2} sequence, which was derived from a *pCreER*^{T2}*-SV40pA* plasmid, at the EcoRI site of a

pCXLE-EGFP plasmid (addgene 27082). Hybrid primers (Pthlh-hyb Fw: GAGAGCCGGGACTGACCCTCGGGTTCCACTCTTGCAGGTCCCCAGAGCCAGCGAGCGGCACGCCACCATGTCCAATTTACTGACC, Pthlh-hyb Rv: CCCCTCACCCCAGGAGGAAGACCGGTACTTACAGCCTGCGGCCAAGCCCCTCCACCGAACGCGCTATGACCATGATTACGCCAAG) containing 62bp homology arms specific to exon2 of the *PTHrP* gene were used to PCR-amplify the targeting construct from the CEWrAfN plasmid, using CloneAmp HiFi PCR Mix (Clontech). The PCR product was gel-purified prior to electroporation into *E.coli* strain SW105 containing RP23-27F7. Recombinants were selected on bacterial plates containing kanamycin and PCR-screened for homologous recombination events. The Neo^R cassette was removed from correctly targeted BAC clones by L-arabinose induction of *flpe* recombinase, and *lox* sites (*loxP* and *lox511*) in the BAC plasmid were replaced with Amp^R and Neo^R cassettes by recombineering. The modified BAC clone was verified by sequencing high-fidelity long-range PCR products and standard southern blot analysis, and purified by NucleoBond BAC 100 (Clontech) prior to injection. The concentration of the BAC construct was verified on gel. The BAC clone was microinjected into B6SJLF1 fertilized eggs at a concentration of 1 ng/µl. Genomic DNA from potential founders was genotyped with PCR primers (387: CAGTTAGAGGCGCTGATTCC, 22: ATTCTCCCACCGTCAGTACG, 810bp), in which one primer is designed external to homology arms while another primer is designed internal to the transgene. Generic *cre* primers (62: CGTACTGACGGTGGGAGAAT, 63: TGCATGATCTCCGGTATTGA, 373bp) were also used. The G0 founder mouse was backcrossed with C57/BL6 mice at least for four generations before analysis.

Histology and immunohistochemistry.

Samples were dissected under a stereomicroscope (Nikon SMZ-800) to remove soft tissues, and fixed in 4% paraformaldehyde for a proper period, typically ranging from 3 hours to overnight at 4^{o}C, then decalcified in 15% EDTA for a proper period, typically ranging from 3 hours to 14 days. Decalcified samples were cryoprotected in 30% sucrose/PBS solutions and then in 30% sucrose/PBS:OCT (1:1) solutions, each at least overnight at 4^{o}C. Samples were embedded in an OCT compound (Tissue-Tek, Sakura) under a stereomicroscope and transferred on a sheet of dry ice to solidify the compound. Embedded samples were cryosectioned at 16µm using a cryostat (Leica CM1850) and adhered to positively charged glass slides (Fisherbrand ColorFrost Plus). Cryosections were stored at -20^{o}C in freezers until use. Sections were postfixed in 4% paraformaldehyde for 20 min. For immunostaining, sections were permeabilized with 0.25% TritonX/TBS for 30 min, blocked with 3% BSA/TBST for 30 min and incubated with rabbit anti-periostin (POSTN) polyclonal antibody (1:2,000, EMD-Millipore, ABT280), rat anti-CD200 monoclonal antibody (1:500, Abcam, ab33734) or rabbit anti-cytokeratin 5 (CK5) polyclonal antibody (1:200, Abcam, ab24647) overnight at 4^{o}C, and subsequently with Alexa Fluor 488-conjugated donkey anti-rabbit IgG (A21206) or Alexa Flour 633-conjugated goat anti-rat IgG (A21094) (1:400, Invitrogen) for 3 hours at 4^{o}C. Sections were further incubated with

DAPI (4',6-diamidino-2-phenylindole, 5μg/ml, Invitrogen D1306) to stain nuclei prior to imaging. Stained samples were mounted in TBS with No.1.5 coverslips (Fisher).

RNAscope *in situ* hybridization.

Samples were fixed in 4% paraformaldehyde overnight at 4°C, decalcified in 15% EDTA for 3 – 6 hours and cryoprotected. Frozen sections at 16μm were prepared on positively charged glass slides. *In situ* hybridization was performed with RNAscope 2.5 HD Reagent kit Brown (Advanced Cell Diagnostics 322300) using following probes: *Pthlh* (456521), *Mef2c* (421011) and *Cd200* (518601) according to the manufacturer's protocol.

Tamoxifen.

Tamoxifen (Sigma T5648) was mixed with 100% ethanol until completely dissolved. Subsequently, a proper volume of sunflower seed oil (Sigma S5007) was added to the tamoxifen-ethanol mixture and rigorously mixed. The tamoxifen-ethanol-oil mixture was incubated at 60°C in a chemical hood until the ethanol evaporated completely. The tamoxifen-oil mixture was stored at room temperature until use.

Cell proliferation assay.

To evaluate cell proliferation, 5-ethynyl-2'-deoxyuridine (EdU) (Invitrogen A10044) dissolved in PBS was administered twice (6 and 3 hours) before sacrificed at P7 or P14 (dose per injection: 100μg for P7, 200μg for P14). Click-iT Imaging Kit (Invitrogen, C10337) with Alexa Flour 647-azide (Invitrogen A10277) was used to detect EdU in cryosections.

Imaging.

Images for fixed sections and live cell culture were captured by an automated inverted fluorescence microscope with a structured illumination system (Zeiss Axio Observer Z1 with ApoTome.2 system) and Zen 2 (blue edition) software. The filter settings used were: FL Filter Set 34 (Ex. 390/22, Em. 460/50 nm), Set 38 HE (Ex. 470/40, Em. 525/50 nm), Set 43 HE (Ex. 550/25, Em. 605/70 nm), Set 50 (Ex. 640/30, Em. 690/50 nm) and Set 63 HE (Ex. 572/25, Em. 629/62 nm). The objectives used were: Fluar 2.5x/0.12, EC Plan-Neofluar 5x/0.16, Plan-Apochromat 10x/0.45, EC Plan-Neofluar 20x/0.50, EC Plan-Neofluar 40x/0.75, Plan-Apochromat 63x/1.40. Images were typically tile-scanned with a motorized stage, Z-stacked and reconstructed by a maximum intensity projection (MIP) function. Differential interference contrast (DIC) was used for objectives higher than 10x. Representative images of at least three independent biological samples are shown in the figures.

Cell preparation.

Gingival tissues of detached mandibles were completely removed using sharp forceps, and dentoalveolar components including molars, sockets and dental sacs were carefully resected using a disposable scalpel (No.15, Graham-Field). Molars (M1 and M2) were carefully extracted

from sockets in a 35mm dish containing 3ml Ca^{2+}, Mg^{2+}-free Hank's Balanced Salt Solution (HBSS, Sigma H6648) containing 2 Wunsch units of Liberase TM (Roche), and incubated at 37^{o}C for 15 min. on a shaking incubator (ThermomixerR, Eppendorf). Dental follicle cells were obtained by rigorous pipetting and filtration through a 70µm cell strainer (BD) into a 50ml tube on ice to make single cell suspension. Cells were pelleted and resuspended in appropriate medium for subsequent purposes. For cell culture experiments, cells were resuspended in 250µl culture medium and counted on a hemocytometer.

Flow cytometry.

Dissociated dental follicle cells were stained by standard protocols with the following antibodies (1:500, eBioscience). eFlour450-conjugated CD31 (390, endothelial/platelet), CD45 (30F-11, hematopoietic), Ter119 (TER-119, erythrocytes), fluorescein isothiocyanate (FITC)-conjugated CD90.2 (30-H12, Thy1.2), phycoerythrin (PE)-conjugated CD51 (RMV-7, aV integrin), allophycocyanin (APC)-conjugated CD45 (30F-11), CD105 (MJ7/18, Endoglin), eFlour660-conjugated CD200 (OX90, OX2), peridinin chlorophyll protein complex (PerCP)-eFlour710-conjugated CD200 (OX90). Flow cytometry analysis was performed using a five-laser BD LSR Fortessa (Ex. 405/488/561/640 nm) and FACSDiva software. Acquired raw data were further analyzed on FlowJo software (TreeStar). Representative plots of at least three independent biological samples are shown in the figures.

Three-dimensional surface rendering of computed tomography images.

Scans were exported to DICOM files using the manufacturer's software and analyzed. The original DICOM files (baseline) were converted to de-identified files in gipl.gz format using the ITK-SNAP open-source software(2, 3). A three-dimensional volumetric label map, a.k.a. segmentation was constructed for each sample wherein the mandible, incisor and three molars were marked as separate label map using ITK-SNAP. The semi-automatic segmentations used active contour method to define boundaries of label maps using image grey level and intensity. These segmentations were then converted to 3D surface models in Slicer open source software. Subsequently, using the Q3DC tool in slicer, fiducials were placed on the mandibular 1st molar, 2nd molar and inferior border of the mandible. Fiducials were placed on the inferior most point on the border of the mandible a.k.a Menton. For the 1st molar, fiducial placement was on the inferior-most point on the mesial and distal root; the most concave point in the furcation; the most convex point on the buccal, lingual, mesial and distal surfaces; as well as the cusp tip of mesiobuccal, distobuccal and mesiolingual cusp tips. Similar landmarks placed on the 2nd molar and 3rd molars. Quantitative measurements were made in Slicer by measuring the line distance between fiducials. To compare the height of eruption, distance between Menton and inferior-most point on the 1st molar root was compared between Control, DF-PPR cHet and DF-PPR cKO samples. Another measurement to assess under-eruption was to analyze the distance between Menton and molar cusp tips. To assess the crown morphology, the mesiodistal and buccolingual width of the 1st mandibular molar was measured and compared between Control,

DF-PPR cHet and DF-PPR cKO samples. The distance between the cusp tip and molar root was measured to compare the molar root length between samples. The interseptal bone was assessed by measuring the distance between the midpoint of a line connecting the inferior point on mesial and distal root; to the fiducial in the furcation. For visual superimposition, the surface models for littermate knockout and het sample overlays were created using the transforms tool in Slicer. Inferior border of the mandible and condylar head were used as matrix. For patients' 3D-CBCT data, the initial step was to create a head orientation matrix for overlay; due to bilateral mandibular asymmetry, it was determined to orient the images based on the cranial base. A three-dimensional volumetric label map a.k.a. segmentation was constructed for each patient, wherein the cranial base, maxilla, mandible and teeth were marked as one single label map using ITK-SNAP program. This full-face segmentation was used to create a surface model for the 3D label map using model maker tool in Slicer software. The full-face surface model was then oriented via three planes in the 3D coordinate system - Frankfort horizontal, mid-sagittal and trans-porionic using following reference points. The mid-sagittal plane was determined by glabella and crista galli, the Frankfort horizontal plane by right, left porion and left orbitale; and the trans-porionic plane by a line passing through right and left porion perpendicular to the Frankfort horizontal plane. An orientation matrix was thus created for this head orientation using the transforms tool in Slicer, and this matrix was applied to the original scan. Then, all subsequent patient segmentations and surface models were oriented. Next, three-dimensional volumetric label maps a.k.a. segmentations were constructed for each patient, wherein the maxilla, mandible and teeth were separate label maps using ITK-SNAP program. Two such separate segmentation files were created to label hemisections of mandible for the affected and unaffected side. The semi-automatic segmentations used active contour method to define boundaries of label maps using image grey level and intensity. These segmentations were then converted to 3D surface models in Slicer software. The original files (scan, segmentation and surface models) were mirrored to allow the superimposition and the evaluation of the differences between affected and unaffected sides. Finally, the original and mirrored files were registered using voxel-based registration in Slicer software. The regional maxillary and mandibular registrations were performed to visually evaluate differences between affected and unaffected sides.

Statistical analysis.

No statistical method was used to predetermine sample size. Sample size was determined on the basis of previous literature and our previous experience to give sufficient standard deviations of the mean so as not to miss a biologically important difference between groups. The experiments were not randomized. All of the available mice of the desired genotypes were used for experiments. The investigators were not blinded during experiments and outcome assessment. Genotypes were not particularly highlighted during quantification.

References for Supplemental Methods

1. Mizuhashi K*, et al.* (2018) Resting zone of the growth plate houses a unique class of skeletal stem cells. *Nature* 563(7730):254-258.
2. Cevidanes LH, Styner M, & Proffit WR (2009) [Three-dimensional superimposition of the skull base for the longitudinal evaluation of the effects of growth and of treatment]. *Orthod Fr* 80(4):347-357.
3. Ruellas AC*, et al.* (2016) 3D Mandibular Superimposition: Comparison of Regions of Reference for Voxel-Based Registration. *PLoS One* 11(6):e0157625.